	ITTC – Recommended Procedures and Guidelines		7.5-03 04 - 01 Page 1 of 24
	Guideline on Use of RANS Tools for Manoeuvring Prediction		Effective Date 2024 Revision 03

ITTC Quality System Manual Recommended Procedures and Guidelines

Guideline

Guideline on Use of RANS Tools for Manoeuvring Prediction

7.5	Process Control
7.5-03	CFD
7.5-03-04	Manoeuvrability
7.5-03-04-01	Guideline on Use of RANS Tools for Manoeuvring Prediction

Disclaimer

All the information in ITTC Recommended Procedures and Guidelines is published in good faith. Neither ITTC nor committee members provide any warranties about the completeness, reliability, accuracy or otherwise of this information. Given the technical evolution, the ITTC Recommended Procedures and Guidelines are checked regularly by the relevant committee and updated when necessary. It is therefore important to always use the latest version.

Any action you take upon the information you find in the ITTC Recommended Procedures and Guidelines is strictly at your own responsibility. Neither ITTC nor committee members shall be liable for any losses and/or damages whatsoever in connection with the use of information available in the ITTC Recommended Procedures and Guidelines.

Prepared by	Approved
Manoeuvring Committee of the 30 th ITTC	30 th ITTC 2024
Date 7/2023	Date 09/2024



	ITTC – Recommended Procedures and Guidelines		7.5-03 04 - 01 Page 2 of 24
	Guideline on Use of RANS Tools for Manoeuvring Prediction		Effective Date 2024 Revision 03

Table of Contents

1. PURPOSE OF GUIDELINE.....	3	2.2.1 Motion equations of the ship	9
2. SIMULATION APPROACH	3	2.2.2 Coupling of ship motions & flow ..	10
2.1 General Considerations	3	2.3 Simulation of Forced Motions	10
2.1.1 Scale	3	2.3.1 Forced ship motions	10
2.1.2 Governing Equations of the Fluid	3	3. SIGNIFICANT PARAMETERS.....	10
2.1.3 Turbulence Model.....	4	4. EXAMPLES.....	11
2.1.4 Propulsion and Steering Model....	4	4.1 Direct Manoeuvring Simulation	11
2.1.5 Computational Grid.....	5	4.2 Simulation Based on Derivatives ...	17
2.1.6 Coordinate Frame.....	6	5. SYMBOLS.....	22
2.1.7 Boundary Conditions	7	6. REFERENCES	22
2.1.8 Free surface treatment.....	8		
2.1.9 Flow current.....	8		
2.2 Direct Manoeuvring Simulation	8		

	ITTC – Recommended Procedures and Guidelines		7.5-03 04 - 01 Page 3 of 24
	Guideline on Use of RANS Tools for Manoeuvring Prediction		Effective Date 2024 Revision 03

Use of RANS Tools for Manoeuvring Prediction

1. PURPOSE OF GUIDELINE

Reynolds Averaged Navier Stokes (RANS) turbulence model can be applied to predict the manoeuvring behaviour of a vessel. This can be achieved either by using a RANS code for predicting the trajectory and more in general, the 6 Degrees of Freedom (DOF) motion due to the movement of an appendage such as the rudder directly, or by calculating the hydrodynamic forces and moments acting on the ship or ship model during simulations with imposed motions. The latter results can be used to determine manoeuvring derivatives (named hydrodynamic coefficients) for manoeuvring predictions.

A description of different techniques is presented from the practical point of view, together with recommended practices to obtain feasible manoeuvring prediction results. The numerical techniques used to discretise the involved partial differential equations, e.g. finite difference method or finite volume method, to model the turbulence of the flow and to generate grids have been described in many publications (e.g. Anderson et al., 1984; Blazek, 2001; Ferziger and Peric, 2002; Hirsch, 1988; Wilcox, 1993).

The present guideline is mainly focused on surface ships in unrestricted calm waters, where usually only four degrees of freedom (surge, sway, yaw, roll) are relevant for manoeuvring. In revision 01 some considerations were added for shallow or restricted water conditions.

2. SIMULATION APPROACH


2.1 General Considerations

2.1.1 Scale

In principle RANS simulations can be applied to full scale ships, avoiding any scale effects. In practice however, most simulations are performed for the ship model scale rather than the full-scale ship because computations for Reynolds numbers of the order 10^9 are not fully validated yet. Full scale simulation yields much more numerical difficulties than for Reynolds number at model scale which is normally 2 orders of magnitude smaller than full scale. In addition, prediction results for the model can be evaluated by comparing them with the results of a few selected free model tests. This “hybrid” prediction procedure seems especially attractive for towing tanks.

2.1.2 Governing Equations of the Fluid

The Navier-Stokes (NS) equations and the continuity equation describe the conservation of momentum and mass in a viscous turbulent incompressible flow and are best suitable to describe the flow around a ship. In order to work with mean values of all flow variables (e.g. velocities, pressure) instead of instantaneous values, the RANS equations are obtained by averaging the NS equations. This averaging can be seen as time averaging in case of a steady mean flow, but has to be understood as ensemble averaging in case of an unsteady mean flow (e.g. Wilcox, 1993; Cebeci et al., 2005). As a result of the averaging, the RANS equations contain some new unknown terms representing the effect of the turbulence on the mean flow. In order

	ITTC – Recommended Procedures and Guidelines		7.5-03 04 - 01 Page 4 of 24
	Guideline on Use of RANS Tools for Manoeuvring Prediction		Effective Date 2024 Revision 03

to solve the set of conservation equations, these terms are approximated by a turbulence model. The reason for doing so is that if not, the required space and time resolution for solving the NS equations directly would be impracticable (probably still in the next decades) for a turbulent ship flow.

2.1.3 Turbulence Model

Any turbulence model used by usual RANS applications can also be used for manoeuvring tasks. The most popular models are the family of k - ϵ / k - ω SST models (Launder et al., 1975; Launder and Spalding, 1974; Wilcox, 1993; Menter et al., 2003) and several variants primarily using wall functions, which allow a significant coarser resolution of near wall regions.

Other models like explicit algebraic stress models, detached eddy simulation (DES) models or one equation models are also applied for manoeuvring computations (SIMMAN 2014).

When looking for prediction of complex flow phenomena however, e.g. detailed flow separation, none of the turbulence models can accurately predict all aspects of the flow with current grids and solvers (Abdel-Maksoud et. al 2015 and Franceschi et. al 2021).

Results presented at the CFD Workshops held in Gothenburg (2010) and Tokyo (2015) have shown a strong dependency for both the resistance and the velocity field on the turbulent model, however, the experience from published results and workshops shows that the dependence of the turbulence model on side force and yaw moment, i.e. the forces which are most significant for manoeuvring, is less significant (Abdel-Maksoud et al., 2015). One possible reason is that these hydrodynamic forces are certainly viscosity dependent but primarily dominated by pressure. In fact, satisfactory results can be achieved even using wall functions as


they do not deteriorate the quality of the predictions to the same extent as when predicting resistance.

2.1.4 Propulsion and Steering Model

Disregarding cases where RANS tools are used for predicting forces on the bare hull only, e.g. to determine coefficients for hull forces in a modular mathematical model, the appendages must be taken into account for manoeuvring simulations. Inclusion of rudders and even bilge keels has become usual in RANS applications. This complicates the grid generation and probably also some flow aspect, which can lead to increased convergence difficulties (such as the appendage accuracy with respect to the selected grid). Nevertheless, the presence of the appendages is fundamental to be considered in the evaluation of the ship manoeuvring capabilities.

The main issue is how to treat the propeller(s), which is crucial for simulating the rudder inflow correctly when rudders are placed behind propellers. Taking the real geometry of the propeller into account and considering the rotating propeller during the RANS simulation is possible (Carrica and Stern, 2008; Aram and Mucha, 2023) but extremely time consuming. Thus, body forces, which are added to the right-hand sides of the RANS equations, are frequently used to approximate the effect of the propeller on the flow (Franceschi et. al 2022). These forces are distributed over the grid region corresponding to the spatial position of the propeller so that the propeller thrust and torque can be computed.

Body force models, mostly based on potential flow codes, such as vortex-lattice or panel methods are often used for approximating the propeller effect including slip stream and swirl. This may also influence aspects of the flow like rudder stall angle, risk of cavitation, etc. The body force distribution inside the propeller region may be calculated in every new time step

 INTERNATIONAL TOWING TANK CONFERENCE	ITTC – Recommended Procedures and Guidelines		7.5-03 04 - 01 Page 5 of 24	
	Guideline on Use of RANS Tools for Manoeuvring Prediction		Effective Date 2024	Revision 03

or in some larger time intervals, based on the propeller inflow obtained during the RANS simulation and the propeller rpm. This can be achieved either interactively, running the potential code each time step, or determining the forces in grid cells within the propeller region from a data base calculated beforehand for the considered propeller. Figure 1 shows the cylindrical body force region (rectangle) and the effect of the body forces on the axial velocity in the longitudinal central plane.

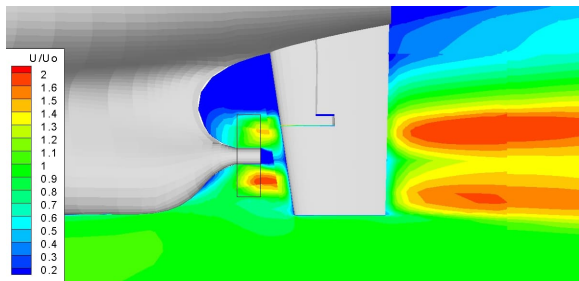


Figure 1 Body force region and effect on the flow

The choice of the propulsion point, corresponding to the full scale or to the model scale, should be decided following similar criteria as for model tests (see procedure 7.5-02-06-02). A way for determining the correct propeller rpm before starting the manoeuvre simulation is to calculate the flow for the steady straight ahead motion of the ship at the given approach speed for different rpm's and to determine the one which makes the total longitudinal force equal to the desired value (e.g. zero or estimated skin friction correction force). The drawback of this method to find the self-propulsion point in CFD is that several runs at different RPS have to be performed. These computations are very resource intensive and take a long time. On the other hand, a speed controller can be applied, which can vary the propeller revolution with different control algorithm. The self-propulsion point can be found during a single simulation.

A proper strategy for the propeller rpm during the manoeuvre, resembling the real behaviour in full scale where the rpm often varies depending on torque, can also be implemented.


The choice of propeller model can have a significant effect on the manoeuvring simulation results as the body force propeller does not consider the lateral propeller forces (Sadat-Hosseini et al., 2014; Broglia et al., 2011; Aram and Mucha, 2023). Lateral forces should be included to get more accurate results.

2.1.5 Computational Grid

Commercial grid generators are widespread, but also open source software is getting more popular recently. Block-structured grids, often including non-matching interfaces, and unstructured grids with several millions cells have become usual for manoeuvring applications.

Contrary to many CFD applications for ship resistance or propulsion, the nature of the problem now requires a grid covering the surroundings at both sides of the ship.

In line with the actual best practices, the grid convergence study (and time-step one, if necessary) has to be performed to assess the Uncertainty Analyse of the selected code setup. Most of the more recent reference literature shows these kinds of studies, but the comparison with experimental measurements is still scarce and limited only to literature available data. Despite these aspects, monotonic convergence is often easy to achieve for bare hull configuration, but it becomes more challenging when fully appended configuration or strongly non-linear regions are considered. Not only for turning the propeller but also to deflect the rudder within direct manoeuvring simulations, a RANS code with sliding grid or overlapping grid capability is needed (Carrica et al., 2013; Muscari, 2008 and Durante, 2010). In the later case a considerable amount of computational effort is required

 <small>INTERNATIONAL TOWING TANK CONFERENCE</small>	ITTC – Recommended Procedures and Guidelines		7.5-03 04 - 01 Page 6 of 24
	Guideline on Use of RANS Tools for Manoeuvring Prediction		Effective Date 2024 Revision 03

for transferring flow information from one grid part to the other. Otherwise, and whenever possible, the grid is kept unchanged during the computation in order to not deteriorate its quality which directly influences the convergence behaviour and the quality of the results. However, this is obviously not possible in many cases of interest for example when considering squat in shallow water or approaching a quay. In such cases a suitable grid deformation technique can be an alternative to overlapping grids (Ji, 2010).

The grid can be generated in several ways and many different grid topologies can be chosen. Any choice can be considered valid as long as the resolution in the near and far field is enough to model the main flow characteristics (such as propagated waves or ship wake). The outer boundaries of the grid mostly consist in planes delimiting a box (hexahedron) surrounding the ship. Figure 2 shows a typical configuration for a manoeuvring application for a double body in deep water. Other strategies and domain shapes can be adopted with proper boundary conditions.

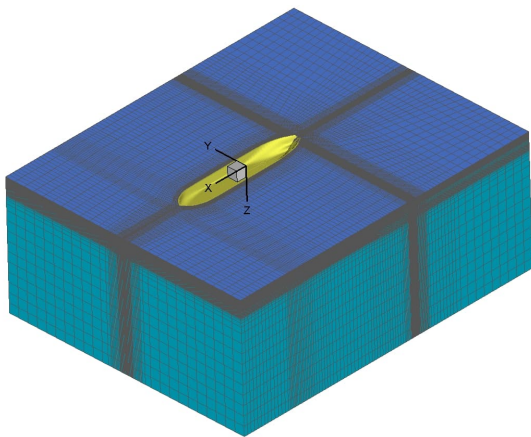


Figure 2: Grid and boundaries of hexahedral computational domain

The grid has to cover the flow domain of interest in such a way that non-physical boundaries (see 2.1.7) are far away of the region of interest, i.e. the ship vicinity. Typical dimensions of a

grid are 3-5 ship lengths in longitudinal direction, 2-3 in transverse direction and one length in vertical direction for deep water.

The near wall region has to be meshed so that the requirements of the used turbulence model are fulfilled (e.g. Wilcox, 1993; Menter et al., 2003). In any case, a certain number of grid points within the boundary layer have to be placed dependent on the turbulence model. For the reasons mentioned in subsection 2.1.3 regarding the influence of viscosity on side force and yaw moment, wall functions are often used for manoeuvring cases.


For shallow and restricted water, the grid has to be dense enough to propagate the wave and pressure field and resolve possible boundary layers in the surrounding environment. On vertical walls and bottom surfaces wall functions may be used to avoid large grid densities. The grid size is defined accordingly to the wall function.

In case waves are included in the simulation, the grid size near the free surface should be defined accordingly to the wavelength and height.

2.1.6 Coordinate Frame

If the flow computation is made in a ship fixed coordinate frame, i.e. if the conservation of momentum is stated in terms of its components in a ship fixed coordinate system, inertial body forces, e.g. centrifugal and Coriolis forces, have to be added to the RANS equations. These forces are usually treated explicitly during the computation and could affect the stability and convergence of the computation if they are considerably larger than the hydrodynamic forces themselves.

On the other hand, if the flow computation is made in an earth fixed or inertial coordinate frame, no inertial forces have to be added but

 INTERNATIONAL TOWING TANK CONFERENCE	ITTC – Recommended Procedures and Guidelines		7.5-03 04 - 01 Page 7 of 24
	Guideline on Use of RANS Tools for Manoeuvring Prediction		Effective Date 2024 Revision 03

cell boundary velocities will have to be considered in order to calculate the correct mass and momentum fluxes through the cell sides; see for instance Ferziger and Peric (2002). Both procedures are mathematically equivalent. The numerical advantages of one or the other procedure seem not significant for typical manoeuvring applications.

2.1.7 Boundary Conditions

The boundary conditions (BC) are crucial for the accuracy of the numerical solution. Setting non-physical boundary conditions such as undisturbed flow (Dirichlet) or zero-gradient (Neumann) too close to the ship will affect the results. The way BC are imposed within the numerical technique may change from code to code but does not differ for manoeuvring tasks from other applications. However, during manoeuvring simulations there are often no longer unambiguous inlet or outlet borders of the computational domain but mixed forms.

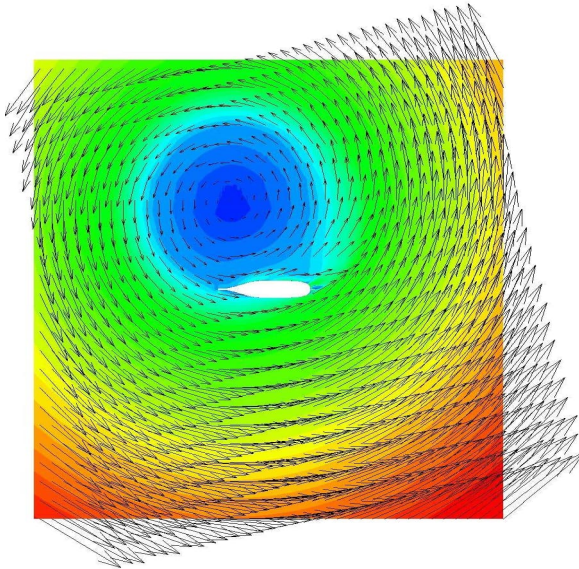


Figure 3: Velocities in horizontal plane around a ship in steady turning to starboard with drift angle 22°

In unsteady flow cases, the BC may have to be updated during the simulation according to the instantaneous ship motion.

At an “inlet” border for instance, far in front of the ship (e.g. 1 L_{pp}) the absolute velocity is zero (in absence of current and waves).

Within a ship fixed frame however, inlet velocities are relative velocities. It is of equal magnitude but opposite to the velocity of the point on boundary from the translation and rotation of the ship fixed coordinate system:

$$\mathbf{u}_{\text{inlet}} = -(\mathbf{u} - \mathbf{y} \mathbf{r})$$


$$\mathbf{v}_{\text{inlet}} = -(\mathbf{v} + \mathbf{x} \mathbf{r})$$

A pressure BC, either zero pressure for double body flow or undisturbed hydrostatic pressure distribution for free surface flow, has proven to be advantageous for the “outlet” border far behind the ship (e.g. 2-4 L_{pp}).

At the sides of the computational domain, e.g. placed 1-2 L_{pp} away from the ship, the velocities may also be given, but these borders could also be treated as inlet and outlet boundaries, for instance in case of a steady oblique towing motion at large drift angle.

At rigid walls like the hull, a “no slip” BC is mostly set, ensuring that the fluid particles have the same velocity as the wall. Sometimes however, it is convenient to consider a wall without any friction, a “free slip” wall, for instance to delimit the computational domain. Note that, if planar, such walls behave similar to symmetry planes.

The bottom of the computational domain can be seen as a free slip wall placed far below the ship for deep water (e.g. one L_{pp}). Same can be chosen for the top border of the considered hexahedral domain, placed at the waterline in case of double body flow or at some distance (e.g. 0.5

	ITTC – Recommended Procedures and Guidelines		7.5-03 04 - 01 Page 8 of 24
	Guideline on Use of RANS Tools for Manoeuvring Prediction		Effective Date 2024 Revision 03

L_{pp}) above the waterline in case of a free surface flow.

For shallow water the bottom is mostly treated similar to the rigid walls mentioned above, i.e. a no slip BC or a moving no slip BC, depending on the simulation approach, is set to ensure the fluid particles have the same velocity as the bottom.

Note that during manoeuvres (when a free-model test is considered) often no real inlet and outlet boundaries exist and a border of the computational domain may change its character during the simulation. For these reasons some adapted “mixed” BC taking this feature into account have proven to be very advantageous. Hereby the velocities are given if the flux is directed into the domain only and they are let free otherwise. This has been done at the left, upper and lower lateral borders in the example of Figure 3, while undisturbed pressure was assumed at the right border. The calculated velocity field differs from the undisturbed field in the close vicinity of the ship only.

2.1.8 Free surface treatment

Computations can be performed taking the water free surface into account or not. The latter approach is reasonable for a slow ship in deep water and requires significantly less computational effort (e.g. factor 10). However, even at low Froude numbers, the underwater shape and thus the forces could change significantly if the sinkage and trim of the vessel vary at large drift angle or yaw rate. A way to take such changes into account would be including the free surface and using a 6 DOF motion model (see below) letting the ship free to sink and trim during the simulation. Other strategies can be considered to take into account the ship's attitude, such as a stepped ship motion obtained evaluating the equilibrium after a fixed time/iteration interval. This approach can, in particular conditions, save computational time and reduce the effect of the

flow oscillation on the results (Franceschi et. al 2021).


Including the water free surface which has become more standard recently, leads not only to more computational time but also to increased numerical difficulties. In particular, reflection of the waves generated by the ship on non-physical or open boundaries (outlet) should be avoided. Among other techniques to avoid such reflections, a strong coarsening of the grid towards the outlet has proven to be very efficient in damping the outgoing waves preventing reflections in a rather rude manner. This procedure however would not be applicable if the considered boundary changes its type (e.g. from outlet to inlet) in the course of the simulated manoeuvre.

2.1.9 Flow current

CFD simulations are usually carried out in a uniform current in velocity and direction, which is also the assumption at sea trials. In this case, the current has no influence on the manoeuvring forces or trajectory since motions through water are considered. Consequently, computations can be performed without current. This is less evident in shallow or confined water as the blockage of the vessel will affect the current flow. The current field will have a boundary layer between the bottom of model and the banks, yielding a non-uniform current situation. So far non-uniform current has not been given much attention in CFD simulations. For that specific case, an earth fixed reference frame seems to be the easiest choice (see 2.1.6).

2.2 Direct Manoeuvring Simulation

Rudder manoeuvres like zig-zag tests and turning circle tests are simulated by solving together the motion equations of the ship, considered as a rigid body, and the RANS equations for the fluid. The rudder(s) is (are) turned according to the desired manoeuvre during the

 <small>INTERNATIONAL TOWING TANK CONFERENCE</small>	ITTC – Recommended Procedures and Guidelines	7.5-03 04 - 01 Page 9 of 24	
		Effective Date 2024	Revision 03

simulation. This kind of manoeuvring simulation is extremely time-consuming but, since there is no mathematical model for the hydrodynamic forces involved, in principle easier than by means of manoeuvring derivatives. It will represent the best approach once comprehensively validated.

2.2.1 Motion equations of the ship

In order to predict the manoeuvre, the rigid motion equations of the ship in 3-DOF, 4-DOF or even in 6-DOF are numerically integrated in time with a proper discretisation scheme, e.g. Euler implicit, Runge-Kutta, etc. In most applications, provided large accelerations are not expected, the Euler explicit scheme can be used as well. The considered motion parameters should be properly defined by means of an earth-fixed or “inertial” coordinate system, a ship-fixed coordinate system and/or with help of an intermediate or “hybrid” coordinate system to uniquely define angles and translations. The singularity (gimbal lock, typically for $\cos\theta=0$) occurring when using Euler angles is not relevant for a surface ship.

An example of motion equations in four degrees of freedom (4 DOF) for a free sailing (rigid) ship or model, written in a hybrid coordinate system which follows the ship motions excepting roll, reads:

$$m[\dot{u} - \dot{\psi}v - x_G^* \dot{\psi}^2 + z_G^* (2\dot{\psi}\dot{\phi}\cos\phi + \ddot{\psi}\sin\phi)] = X$$

$$m[\dot{v} + \dot{\psi}u + x_G^* \ddot{\psi} + z_G^* ((\dot{\psi}^2 + \dot{\phi}^2)\sin\phi - \ddot{\phi}\cos\phi)] = Y$$


$$(I_{yy}\sin^2\phi + I_{zz}\cos^2\phi)\ddot{\psi} + (I_{yy} - I_{zz})\dot{\psi}\dot{\phi}\sin\phi\cos\phi - I_{xz}(\ddot{\phi}\cos\phi - \dot{\phi}^2\sin\phi) + mx_G^*(\dot{v} + u\dot{\psi}) + m z_G^* \sin\phi (\dot{u} - v\dot{\psi}) = N$$

$$I_{xx}\ddot{\phi} - I_{xz}\ddot{\psi}\cos\phi + (I_{zz} - I_{yy})\dot{\psi}^2\sin\phi\cos\phi - m z_G^* \cos\phi (\dot{v} + u\dot{\psi}) = K$$

The surge and sway velocities u and v are the components of the velocity of the chosen ship origin O in the horizontal longitudinal and transversal directions x and y of the hybrid coordinate system, respectively. The Euler angles ϕ and ψ are the rotations around the x - and z -axes respectively and describe the roll and yaw motions of the ship. The dots in the above equations denote time derivatives. m is the mass of the ship or model and x_G^* and z_G^* are the coordinates of the center of gravity G in the ship fixed system. It is assumed that $y_G^*=0$. I_{xx}, I_{yy}, I_{zz} are the moments of inertia about the ship fixed axes through the origin O and I_{xz} is the product of inertia. It is assumed that $I_{xy} = 0$ and $I_{yz} = 0$ (valid for ships that have a longitudinal plane of symmetry). X and Y (longitudinal and side force) are the components in the hybrid system of the external force acting on the ship. K and N (roll and yaw moment) are the components in the hybrid system of the moment of the external forces.

Since heave and pitch motions are neglected, the state of movement of the ship is defined by the position of O (earth fixed coordinates), its velocity vector $(u, v, 0)$, the Euler angles ϕ, ψ and the angular velocity vector $(\dot{\phi}, 0, \dot{\psi})$. The time history of these variables can be obtained by integrating the motion equations in time numerically. For this purpose, the hydrodynamic forces and moments on their right-hand sides are needed.

The hydrodynamic forces and moments appearing in the right-hand side of the motion equations are calculated in the course of the time integration by simulating the flow at every new time step. Note that even if heave and pitch are not relevant for manoeuvring prediction in unrestricted water, the ship/model should be free to

	ITTC – Recommended Procedures and Guidelines		7.5-03 04 - 01 Page 10 of 24
	Guideline on Use of RANS Tools for Manoeuvring Prediction		Effective Date 2024 Revision 03

sink and trim during the RANS simulation in order to get the hydrodynamic forces for the most realistic floating condition as possible.

This is easily fulfilled when making simulations with a fully 6-DOF motion model.

Note that it is possible to disable selected motions during the simulations and also to add some external forces, such as skin friction correction force resembling the free model test conditions.

2.2.2 Coupling of ship motions & flow

The coupling between the ship motions and the flow is crucial for determining the hydrodynamic forces. If only moderate ship accelerations are involved (as usual during manoeuvres) this coupling can easily be implemented in an explicit manner: in every new time step of the simulation the RANS code is used to calculate the forces acting on the ship. Subsequently, the motion equations yield the motion parameters for the next time step. Finally, the boundary conditions and inertial forces (if present) are updated before starting a new time step.

2.3 Simulation of Forced Motions

Due to the enormous computational effort required for the direct simulation of manoeuvres described above, another strategy has gained popularity instead. It consists of simulating the usual PMM or CPMC tests numerically, solving the RANS equations around the ship or ship model when performing prescribed motions. Compared to direct manoeuvring simulations, this prediction procedure has the same advantages and disadvantages as between free and captive model tests. From the computational point of view however, it is definitively more robust and less time consuming.

The strategy fully resembles the classical, well accepted PMM tests followed by the determination of derivatives and seems already practicable for commercial applications. Nevertheless, a mathematical model (e.g. a set of coefficients of Abkowitz type (Abkowitz, 1964) or coefficients of formulae for diverse forces of a modular simulation method) is involved, introducing a further source of uncertainty into the prediction.


2.3.1 Forced ship motions

Motion equations are not solved in this case. Selected motions, e.g. harmonic pure sway, pure yaw, etc, are imposed. There are different ways for imposing the motions. In order to resemble CPMC tests or to reproduce measured motions during free model tests, a file containing the time histories for the motion parameters can be as used input. Note that it would be best to let the ship or model free to sink and trim for RANS simulation. The analysis of the predicted time histories, the longitudinal force X , the transverse forces Y , the roll moment K , and yaw moments N should be the same as PMM or CPMC model tests. Moreover, since no artificial time lag between predicted forces and prescribed motions arise and no inertial forces have to be subtracted (no filters, no swinging masses), the analysis is easier than performing model tests.

Similar to model tests, there are different ways of determining the manoeuvring derivatives. The “virtual” test program has to be decided accordingly with different mathematical models (e.g. the derivatives to be determined).

3. SIGNIFICANT PARAMETERS

The first step of any numerical investigation for manoeuvring consists of analysing the considered case and taking decisions like limiting the calculations to double body flow or taking the free water surface into account, considering

	ITTC – Recommended Procedures and Guidelines		7.5-03 04 - 01 Page 11 of 24
	Guideline on Use of RANS Tools for Manoeuvring Prediction		Effective Date 2024 Revision 03

the free sinkage and trim or not, performing the simulations for the ship model or for the full-scale ship. This is followed by the proper choice of a turbulence model, discretisation schemes, grid and time resolution, and the choice of the boundary conditions at the borders of the grid.

In addition, several parameters of the used code have to be chosen as well, for instance: the number of (outer) iterations within each time step, the number of (inner) iterations within an outer iteration, values for diverse under-relaxation factors, among others. Depending on the code, other settings could also be required which may have a strong influence on the result of the computations. For these reasons, experience in viscous flow computations and insight about the RANS code are prerequisites for successful CFD based manoeuvring prediction.

4. EXAMPLES

4.1 Direct Manoeuvring Simulation


With the advancements in numerical methods and increase in computational power, free-running manoeuvring simulations with CFD has gained more interest in recent years. Several studies in the public domain focus on validation of unsteady RANS manoeuvring predictions against experiments. SIMMAN 2020, a workshop on verification and validation of ship manoeuvring simulation methods, offers a rich database for such applications.

Propeller modelling is one of the key elements of hull-propeller-rudder interactions, which may have a significant effect on the predicted manoeuvring simulations. As mentioned in 2.1.4, two common methods for the propeller modelling are the body-force model and the actual propeller (AP) model. In the body-force propeller model, the propeller geometry is excluded, and the propeller thrust is modelled by

adding source terms to the Navier-Stokes equations in the propeller region. The spatial load condition on the propeller blades is not accounted for in this model. Instead, the thrust and torque obtained from the open-water propeller test are used as inputs to the model. On the contrary, the AP method includes the discretization of the propeller geometry and the time-accurate resolution of the rotational motion. As a result, this approach predicts the spatial pressure and wall shear stress distribution over the propeller surface, as well as the swirl and downstream vortical structures which are not predicted in most body force models. A method known as the “frozen rotor” is also available in most CFD software applicable to the propeller modelling, which is built upon the solution of the rotational flow for a discretised propeller region in a moving reference frame (MRF). However, this model is not recommended for the manoeuvring applications, as it is more expensive but not necessarily more accurate than the body-force model.

As an example of the direct manoeuvring simulation, the RANS simulations of turning circle manoeuvres with 25° rudder deflection angle recently published by Aram and Mucha (2023) is presented in this section. The focus of the study was on an evaluation of the two aforementioned propeller models for prediction of local flow field data and principal manoeuvring characteristics applied to the Office of Naval Research Tumblehome (ONRT) surface combatant. The results of both models were compared with the model test data from the University of Iowa Wave Basin Facility, IIHR.

The geometry of the ONRT model 5613 is shown in Figure 4. The model appendages include a skeg, bilge keels, twin rudders, shafts, struts and two 4-bladed propellers. The propeller geometry is excluded for the body-force propeller model (referred to the virtual disk, VD, method). Table 1 summarizes the model partic-

 INTERNATIONAL TOWING TANK CONFERENCE	ITTC – Recommended Procedures and Guidelines		7.5-03 04 - 01 Page 12 of 24
	Guideline on Use of RANS Tools for Manoeuvring Prediction		Effective Date 2024 Revision 03

ulars for a 1/49 scale model. The model geometry can be found on the SIMMAN 2020 site (<https://simman2020.kr/contents/ONRT.php>). The simulations were performed for the scale model to match the model test.

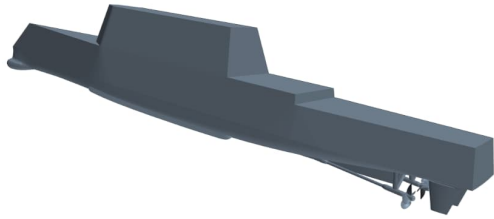


Figure 4: ONRT model 5613

Table 1: Particulars of model scale ONRT 5613

Displacement, Δ (kg)	72.6
Waterline length, L (m)	3.147
Waterline beam, B (m)	0.384
Draft, T (m)	0.112
Wetted surface area, S (m ²)	1.5
Longitudinal center of buoyancy, LCB (m aft of FP)	1.625
Vertical center of gravity, VCG (m from keel)	0.156
Metacentric height, GM (m)	0.0422
Natural roll period, T (s)	1.665
Roll radius of gyration, K_{xx}/B	0.344
Pitch radius of gyration, K_{yy}/L	0.246
Yaw radius of gyration, K_{zz}/L	0.246
Propeller diameter, D_p (m)	0.1066
Propeller shaft angle (deg)	5

Simcenter™ STAR-CCM+ software, a commercial CFD based simulation tool built on volume integral representation of the Navier-Stokes equations (FV method), was employed. In Star-CCM+, mid-point rule is applied for surface and volume integrations representing convective and diffusive fluxes, along with interpolation technique to approximate the cell face values. The segregated solution of the velocity-pressure coupling problem is based on the Semi-Implicit Method for a Pressure Linked Equations (SIMPLE) algorithm. The Volume of Fluid (VOF) method was used to model the free

surface with a High-Resolution Interface Capturing (HRIC) scheme for tracking the sharp interface between water and air. In order to mitigate the wave reflections from the boundaries of the computational domain, the wave damping techniques known as “numerical beaches” was applied. Coarsening the grid resolutions on the free-surface plane was also adopted to further help with the wave reflection damping. The $k-\omega$ Shear Stress Transport (SST) introduced by Menter (1994) was used in this study to model the turbulence. In order to model the ship motions and appendages movements, the overset grid method was employed which allows multiple grids within one computational background domain to overlap arbitrarily.

A rectangular box was used to define the computational domain, which extends $1.5L$ forward of the forward perpendicular, $2.5L$ aft of the aft perpendicular, $2.25L$ from the ship center-plane to the side boundaries, and $2L$ from water-plane to top and bottom boundaries. The Dirichlet boundary condition with zero value for velocity was applied to the boundaries, except the top boundary with pressure outlet as a boundary condition. Ship motions, forces, and moments were reported in the body-fixed coordinate system with the origin at the centre of gravity, $x+$ toward bow, $y+$ toward port and $z+$ up.

Hexahedral-dominant unstructured-grid topology with prism layers for the boundary layer were used to discretise the computational domain, as illustrated in Figure 5. The computational domain contains six regions: background, ship, port and starboard rudders, port and starboard propeller (in the case of AP) where ship, rudder and propeller regions are defined as overset regions to allow their relative motions with respect to the background region as well as free motions of the rudders and propellers relative to the ship.

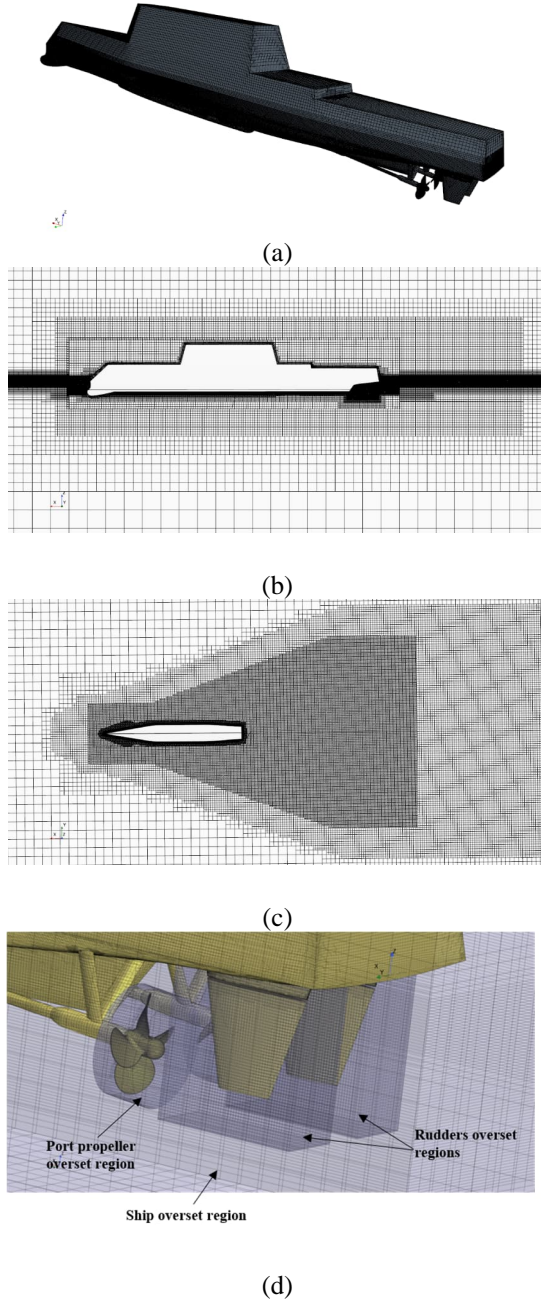


Figure 5: Grid resolution (a) on model surface, (b) volume cut along model center-plane, (c) volume cut along water-plane, and (d) ship, rudders, propeller overset regions

To reduce the computational cost associated with resolving the boundary layer, the wall function is mainly used for practical applications to estimate the flow variables near the solid surface.

In this study, the wall function was applied to the grid with the first prism layer height which results in an averaged y^+ (distance between the first cell centre and solid surface, in viscous units) of ~ 40 . Multiple volume refinement zones were used in the regions with large gradients of flow variables to meet the grid resolution requirements and obtain a smooth transition of boundary layer to free stream. As a general practice, grid sensitivity analysis is recommended to perform in order to achieve flow predictions independent of the grid resolutions. The total cells of 7.5×10^6 for the VD approach and 8.7×10^6 for the AP model are reported for this study.

The VD method uses the local propeller inflow to calculate the propeller advance ratio (J) at each time step for a given propeller rotational speed and extract the thrust and torque from the imported open-water propeller curve. The basic method follows the approach introduced by Hough and Ordway (1965). The propeller inflow disk in this study is located a distance of 8.5% of propeller diameter ($D_p = 0.1066$ m) upstream of the propeller plane with diameter of 1.08 times D_p .

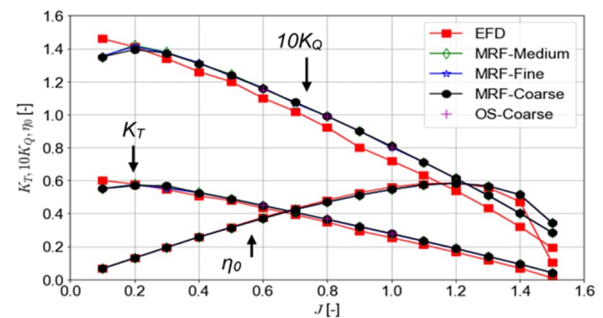


Figure 6: Open water thrust and torque coefficient curves for the port propeller

For the discretised propeller modelling, it is recommended to perform a numerical open-water propeller performance and compare the predicted thrust coefficient (K_T), torque coefficient (K_Q) and propeller efficiency (η_0) with the

available test data.

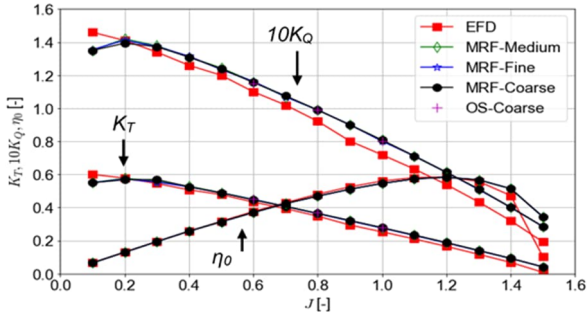


Figure 6 shows this comparison for the ONRT propeller. The MRF technique is suitable for the open-water propeller modelling used in this study. The simulations were performed for three grid resolutions including coarse, medium and fine grid with total cells of 9.5×10^6 , 1.4×10^6 , and 2.7×10^6 , respectively. The plots indicate insensitivity of the predictions to the grid resolutions. The growing difference between CFD and EFD for $J > 0.5$ is primarily related to the turbulence modelling errors as well as uncertainty in EFD partly due to using a plastic propeller with potential to deform.

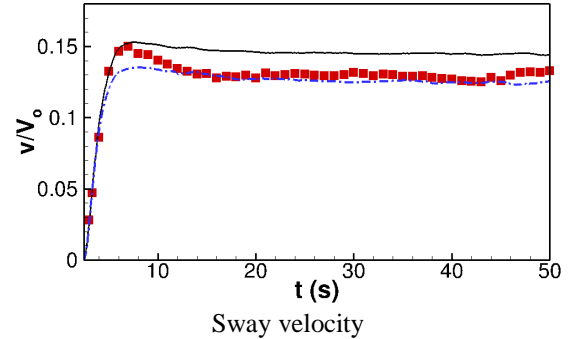
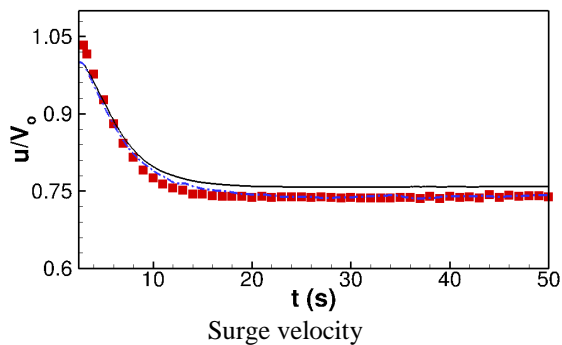
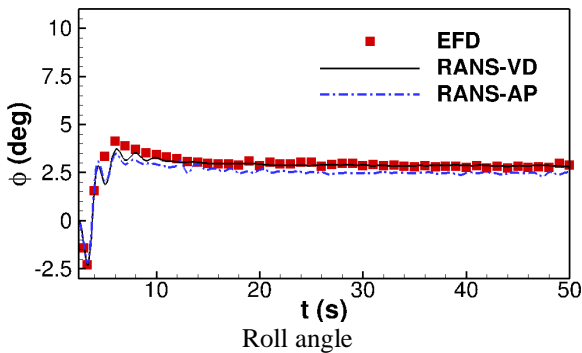


Figure 7: Time history of ship response during port turning circle with 25° rudder angle. Continued

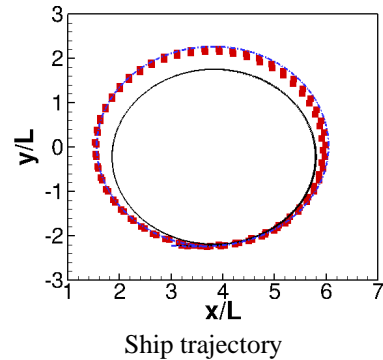
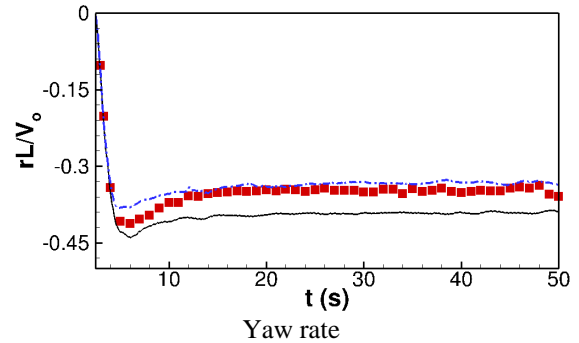



Figure 8: Continued. Time history of ship response during port turning circle with 25° rudder angle

The two-equation eddy viscosity model with isotropic turbulence production assumption used in this study leads to poor accuracy in prediction of separated flows occurring at very low J values. In addition, this turbulence model is not designed to capture the laminar-to-turbulence transition that occurs for small propellers at high advance ratios. Manoeuvring simulations were first performed at the straight-ahead

 INTERNATIONAL TOWING TANK CONFERENCE	ITTC – Recommended Procedures and Guidelines		7.5-03 04 - 01 Page 15 of 24	
	Guideline on Use of RANS Tools for Manoeuvring Prediction		Effective Date 2024	Revision 03

self-propulsion condition to obtain the required propeller rotational speed (n) for achieving the target Froude number of 0.20. Following the British Method (Bertram, 2012), the simulations were conducted for three propeller speeds around the model test value, and the desired propeller speed to reach the target ship speed is identified with a linear interpolation. The interpolated propeller speed is 568.3 RPM for the VD model and 522.6 RPM for the AP model. The propeller speed was kept constant at the value of the self-propulsion point during the turn following the model test.

The time history of selected manoeuvring parameters during the turn with 25° rudder angle is shown in Figure 8 and Figure 8. The results are presented in the model test coordinate system, where $x+$ to bow, $y+$ to starboard, and $z+$ down. The rudder is deflected with 35 deg/s rate to match the model test. The turning circle manoeuvre was initiated at $t_{int} = 2.5$ s in the model test, and the time histories of CFD results were adjusted to match the t_{int} of the model test.

The results of the VD and AP models closely match each other and the model test at the initial phase of the turn, and the VD model starts to deviate from model test data afterwards. The predicted trajectory with the VD model is tighter than the AP model and experiment. In addition, the steady sway velocity and yaw rate are over-predicted with the VD model, while those predicted by the AP model closely correlate with the model test.

Table 2 Manoeuvring characteristics of 25° turning circle

Parameter	EFD	VD	E% VD	AP	E% AP
AD/L	2.89	2.75	-4.84	3.00	3.81
TR/L	1.75	1.64	-6.28	1.89	8
TD/L	4.32	3.80	-12.04	4.46	3.33
$T_{90}Vo/L$	4.41	4.12	-6.58	4.68	6.12
$T_{180}Vo/L$	8.90	8.11	-8.88	9.35	5.06
SD/L	4.39	3.93	-10.48	4.48	2.05
v_{st}/V_o	0.132	0.146	10.61	0.127	3.79

rL/V_o	-0.94	-1.11	18.08	-0.94	0.0
β_{st}, deg	-10.19	-10.83	6.28	-9.60	-5.79

Summary of the key manoeuvring parameters for the model test and simulations are given in Table 2. Except for the transfer (TR/L), the AP model results in a closer prediction to the model test than the VD models. The largest relative error is the drift angle for the VD model and transfer for the AP model. The average magnitude of relative error is 9.34% and 4.22% for VD and AP, respectively.

VD models. During turn, the propeller side force albeit small in magnitude compared to hull forces with values ranging between 10 - 30 % of propeller thrust, acts at virtually the maximum possible distance away from the CG, resulting in a yaw moment that is not negligible in the balance of moments for the turning ship.

The absence of the propeller side force in the VD model in conjunction with the inability to provide the effect of swirl could be the main reasons for the discrepancy between the AP and

With the resulting propeller side forces pointing towards the centre of rotation of the turning circle, a bow-out moment arises, decreases the drift angle of the ship, and results in smaller yaw rates and larger turning diameters.

The inflow velocity components to the rudders on the horizontal plane are compared to the VD and AP models in Figure 9. Index PS is for port, SS for starboard. The axial component of the inflow velocity (u) compares closely between the two models, while the crossflow component (v) is lower for the AP model with the largest relative difference for the port rudder. The discrepancy in the crossflow prediction indicates a lower accuracy of the VD model in modelling the propeller wash flow.

Figure 10 compares the propeller and rudder side force and yaw moment predicted by the AP

model. The propeller force and moment act in opposite direction of those on rudder on port and starboard. Side forces of port and starboard propellers are relatively close, while the yaw moment of port propeller is more than 50 % greater than that of starboard propeller. In addition, the port rudder produces a greater side force and yaw moment than the starboard rudder. The largest error for the VD models is in the yaw rate, which is notably higher than AP model and EFD, and results in a tighter turn.

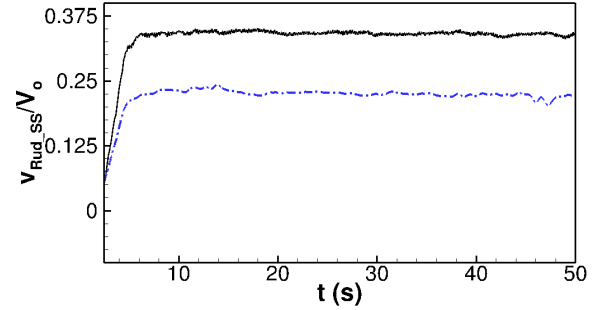
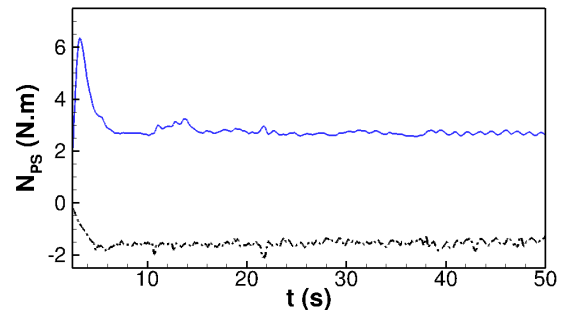
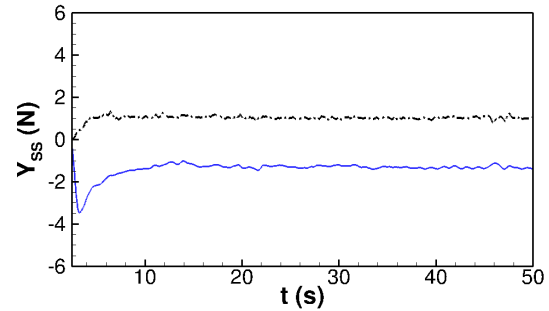
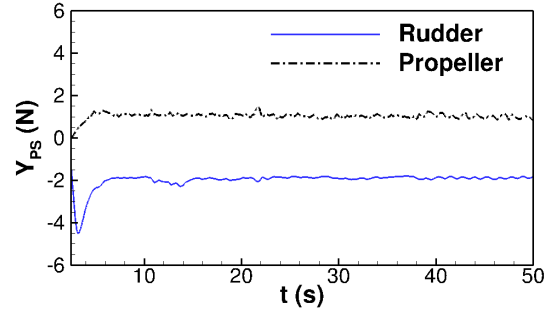
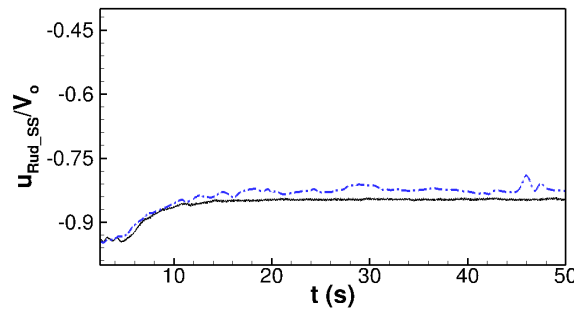
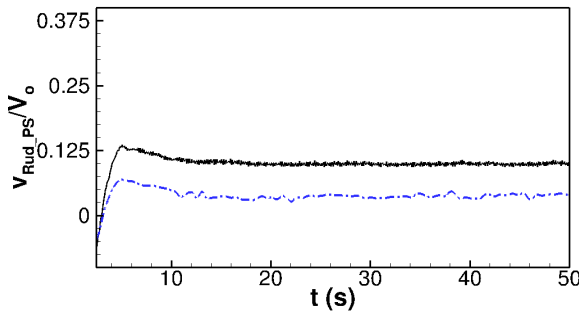
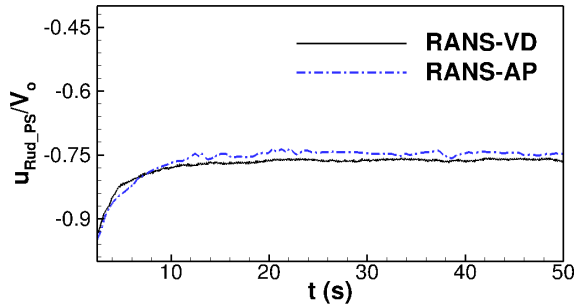


Figure 9: Axial inflow velocity (u) and cross inflow velocity (v) to port and starboard rudders during 25° port turn



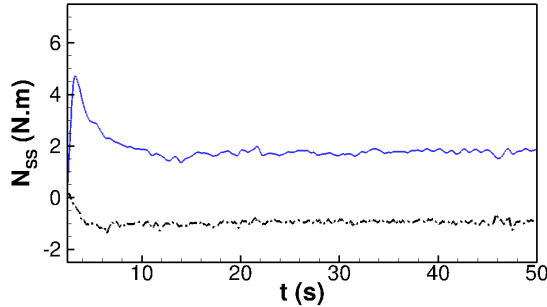


Figure 10: Propeller and rudder side force and yaw moment during 250° port turn

The time-step size for modelling the discretized propeller should be chosen to meet the recommended propeller rotation of $1^\circ - 3^\circ$ per time step, which could be 20 – 30 times of the time step size that can be applied to the body-force models. The resulting computational cost and calculation time of the AP model (weeks of parallel processing) make the use of this model impractical for design applications. Therefore, utilization of higher accuracy body-force models that account for the key elements captured by the discretized propeller model for ship manoeuvring prediction should be the focus of the CFD community.

4.2 Simulation Based on Derivatives

The technique outlined above is applied here to predict the manoeuvrability of a Very Large Crude Carrier (VLCC), namely the tanker KVLCC1, used as a benchmark test in SIMMAN 2008. Due to the low Froude number of the considered tanker and because negligible heel angles are expected during its manoeuvres all RANS simulations are performed without taking the water free surface into account.


A RANS code is used to calculate the flow around the tanker at several static conditions and during virtual pure surge, pure sway, pure yaw and combined sway-yaw tests to obtain a rather simple set of hydrodynamic coefficients of Abkowitz type, see below.

All dynamic tests are simulated using the same multi-block structured grid with about one million cells with (some) non-matching block interfaces. The semi-balanced horn rudder, embedded in an individual grid box, is not deflected during these simulations. For static cases with deflected rudder and constant drift angle and/or yaw rate only this grid box is replaced by another according to the considered rudder angle.

Table 3: Main particulars of KVLCC1

L_{pp}	320.0 m
B	58.0 m
T	20.8 m
∇	312,738 m ³
C_B	0.8101
L_{CB}	3.48 %
GM	5.71 m
i_{xx}/B	0.375
i_{zz}/L_{pp}	0.25
Rudder lateral area	136.7 m ²
Rudder helm rate	2.34 °/s
Ship speed U_0	15.5 kn

The grid dependency of the results must be checked at least by means of selected calculations on different grids. In the present case the values of all forces and moments acting on the ship obtained on coarse medium and fine grids

 INTERNATIONAL TOWING TANK CONFERENCE	ITTC – Recommended Procedures and Guidelines	7.5-03 04 - 01 Page 18 of 24	
	Guideline on Use of RANS Tools for Manoeuvring Prediction	Effective Date 2024	Revision 03

(in scale of $\sqrt{2}$) behaved consistently and differed less than 10% from each other. Although this check cannot replace a real Uncertainty Analysis (UA) it may be a good compromise in practise.

The computations are performed on a ship fixed grid using a Cartesian non-inertial coordinate system. The standard two equations $k-\omega$ turbulence model with wall functions is used. During dynamic tests the motions are imposed through the boundary conditions and corresponding inertial forces added to the RANS equations, see Cura Hochbaum et al. (2008).

The CPU time for a dynamic simulation is still several days per period on a single processor of a normal PC. But it can be much less if a parallel code is run on a cluster with hundreds of processors. The static tests usually take a few hours depending on grid resolution.

Vortex lattice data for the propeller of a typical tanker was used in the present case. The rate of revolutions was set so that the resulting thrust balanced the resistance computed during a steady straight-ahead motion of the model (model self-propulsion point). This rate was kept constant throughout the computations.

Figure 11 shows the velocity distribution just behind the propeller plane during a simulated combined sway-yaw test at a certain time when the ship is turning to starboard. The white circle indicates the body force region.

In order to obtain all manoeuvring derivatives except those depending on the rudder angle and surge velocity, five dynamic tests with large velocity amplitudes and a common non-dimensional period $T' = TU_0/L_{pp} = 3.369$ (20 seconds in model scale) are simulated.

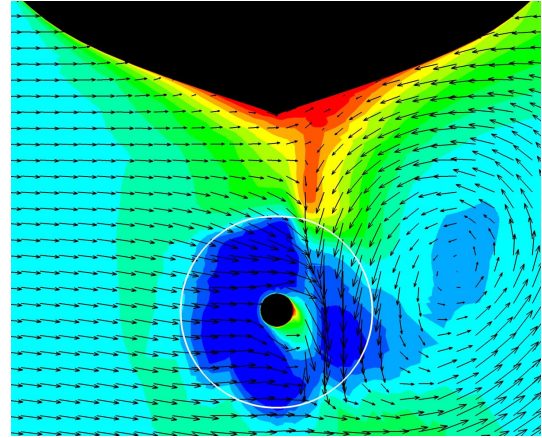
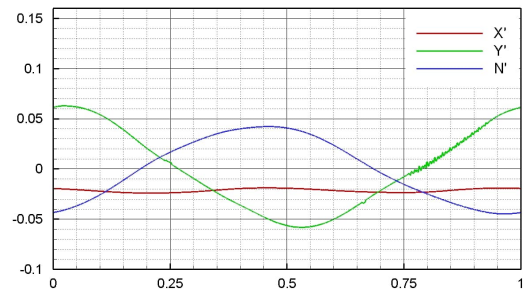
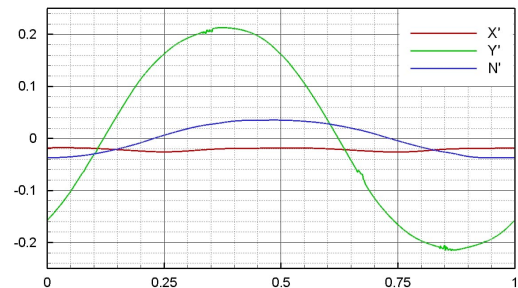


Figure 11: Snapshot of the velocity field behind the propeller during a simulated sway-yaw test

Similar to real tests, the non-dimensional amplitudes of the harmonic motions should be chosen so that they cover the expected range of the motion parameters during the manoeuvres.

In the present example the amplitudes were: $u' = u/U_0 = 0.10$ for pure surge, $v' = v/U_0 = 0.35$ for pure sway, $r' = rL_{pp}/U_0 = 0.70$ for pure yaw and -0.35, 0.20 and -0.20, 0.40 for two combined sway-yaw tests, respectively.



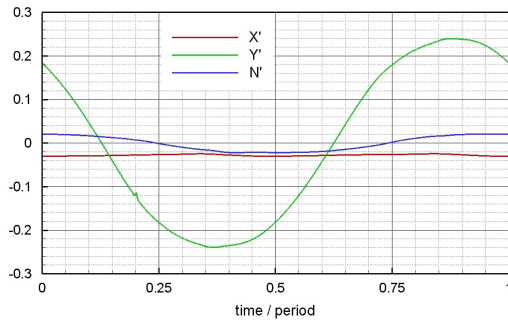


Figure 12: Forces and yaw moment during one period of a virtual pure sway and pure yaw test and a combined sway-yaw test (top to bottom)

The RANS simulations were done for the tanker's model (scale 1:45.7) at a speed of 1.179 m/s. The time step chosen for the RANS simulation corresponded to 1/2500 of the motion period in all cases.

The hydrodynamic forces and moments acting on the ship are obtained by integrating the pressure and shear stresses on the hull and appendages. The predicted time histories during simulated pure sway, pure yaw, as well as combined sway- yaw can be seen in Figure 12. The longitudinal force X' , side force Y' and yaw moment N' have been made non-dimensional with water density, ship speed, length and draught.

Rudder angle depending manoeuvring derivatives can be determined by computing rudder angle tests at several drift angles and yaw rates resulting in a total of 42 cases.

Figure 13 shows the stern arrangement of the virtual model of KVLCC1 with the rudder deflected 35° to starboard. The pressure field on the rudder computed for steady straight-ahead motion is influenced by the effect of the propeller, rotating to the right over the top. Negative pressure regions are depicted in blue, while positive pressure regions are in red.

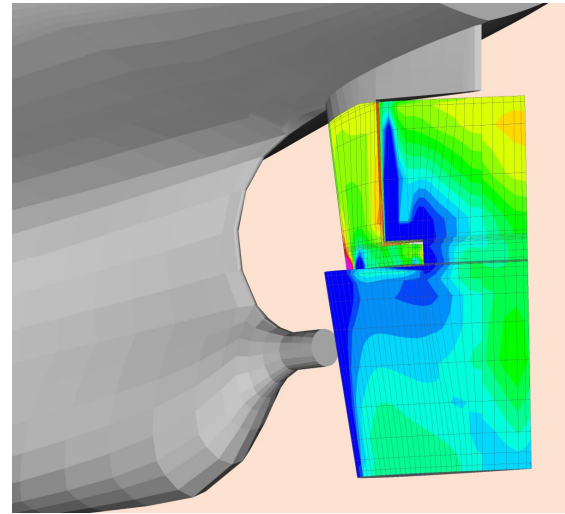


Figure 13: Stern arrangement of the virtual ship model and computed pressure on the rudder deflected 35°

The computed non-dimensional side force and yaw moment acting on the hull for all static cases are summarised in Figure 14 and Figure 15 for oblique towing and steady turning conditions respectively.

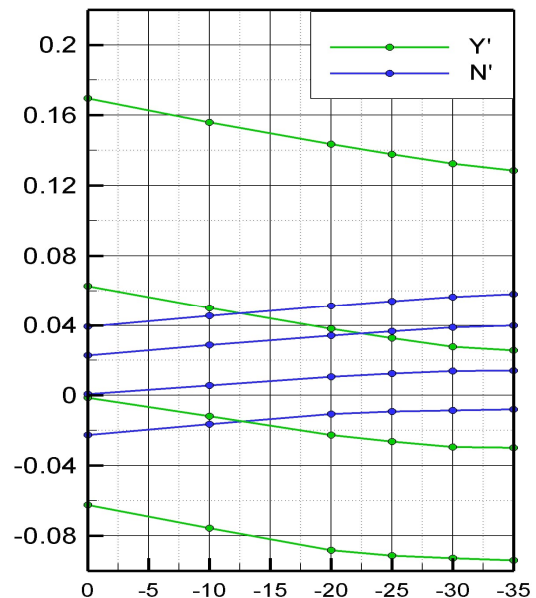



Figure 14: Computed non-dimensional side force and yaw moment during rudder angle tests at drift angle -10° , 0° , 10° and 20°

The time histories of the forces obtained from the RANS simulations for the 5 dynamic

 INTERNATIONAL TOWING TANK CONFERENCE	ITTC – Recommended Procedures and Guidelines		7.5-03 04 - 01 Page 20 of 24	
	Guideline on Use of RANS Tools for Manoeuvring Prediction		Effective Date 2024	Revision 03

tests described above are used to determine the coefficients of the mathematical model in the same way as if PMM tests would have been done. This yields the coefficients in rows 4-18 of Table 4.

Regression analysis of the data obtained from static cases with deflected rudder yields the coefficients depending on the rudder angle written in rows 1-3 and 19-23 in Table 4.

The hydrodynamic coefficients shown in Table 4 have been made non-dimensional with water density, ship speed and length and multiplied by 1000, and are used to simulate standard rudder manoeuvres according to IMO (2002). For this purpose, the motion equations of the ship in four degrees of freedom (4 DOF) were used. However, the dependency of the non-dimensional magnitudes X' , Y' , N' and roll moment K' (not shown) on heel angle and roll rate was neglected since no significant roll motion was expected for the considered tanker. The sub-indices u , v , r and δ denote the surge, sway and yaw velocities and the rudder angle, respectively.

Table 4: Manoeuvring Derivatives

0	X'_o	0	Y'_o	0	N'_o	0
1	X'_δ	0	Y'_δ	4.44	N'_δ	-2.06
2	$X'_{\delta\delta}$	-2.09	$Y'_{\delta\delta}$	-0.24	$N'_{\delta\delta}$	0.16
3	$X'_{\delta\delta\delta}$	0	$Y'_{\delta\delta\delta}$	-2.95	$N'_{\delta\delta\delta}$	1.38
4	X'_u	-2.20	Y'_u		N'_u	
5	X'_{uu}	1.50	Y'_{uu}		N'_{uu}	
6	X'_{uuu}	0	Y'_{uuu}		N'_{uuu}	
7	$X'_\dot{u}$	-1.47	$Y'_\dot{u}$		$N'_\dot{u}$	
8	X'_v	0.11	Y'_v	-24.1	N'_v	-7.94
9	X'_{vv}	2.74	Y'_{vv}	2.23	N'_{vv}	-1.15
10	X'_{vvv}	0	Y'_{vvv}	-74.7	N'_{vvv}	2.79
11	$X'_\dot{v}$		$Y'_\dot{v}$	-16.4	$N'_\dot{v}$	-0.47

12	X'_r	-0.07	Y'_r	4.24	N'_r	-3.32
13	X'_{rr}	0.58	Y'_{rr}	0.56	N'_{rr}	-0.27
14	X'_{rrr}	0	Y'_{rrr}	2.58	N'_{rrr}	-1.25
15	$X'_\dot{r}$		$Y'_\dot{r}$	-0.46	$N'_\dot{r}$	-0.75
16	X'_{vr}	13.1	Y'_{vr}		N'_{vr}	
17	X'_{vrr}		Y'_{vrr}	-40.3	N'_{vrr}	8.08
18	X'_{vvr}		Y'_{vvr}	-9.90	N'_{vvr}	-3.37
19	$X'_{u\delta}$		$Y'_{u\delta}$	-4.56	$N'_{u\delta}$	2.32
20	$X'_{v\delta\delta}$		$Y'_{v\delta\delta}$	5.15	$N'_{v\delta\delta}$	-1.17
21	$X'_{vv\delta}$		$Y'_{vv\delta}$	7.40	$N'_{vv\delta}$	-3.41
22	$X'_{r\delta\delta}$		$Y'_{r\delta\delta}$	-0.51	$N'_{r\delta\delta}$	-0.58
23	$X'_{rr\delta}$		$Y'_{rr\delta}$	-0.98	$N'_{rr\delta}$	0.43

The main results of the simulated 10°/10° zig-zag test starting to starboard are compared with experimental results in Figure 16 which shows the heading angle ψ and the rudder angle δ versus time. The 2nd overshoot angle predicted for KVLCC1 is slightly larger than measured and the overall agreement deteriorates with increasing time. However, the characteristic parameters used to judge yaw checking and initial turning ability are predicted well, Table 5.

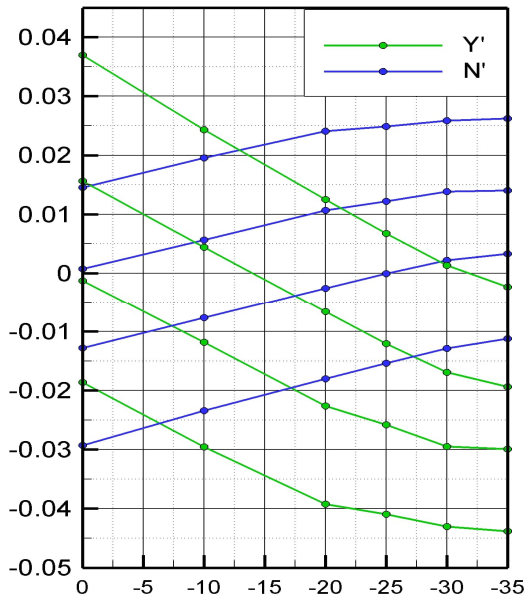


Figure 15: Computed non-dimensional side force and yaw moment during rudder angle tests at non-dimensional yaw rate -0.25, 0, 0.25 and 0.50

Table 5: Characteristic parameters of 10°/10° test

10°/10°	SIM	EXP
time to attain	67 s	69 s
x_{90°	$1.66 L_{pp}$	$1.73 L_{pp}$
α_{01} [°]	8.1°	8.2°
α_{02} [°]	21.4°	19.4°
r_{max}	4.42 °/s	4.40 °/s

Any other rudder manoeuvre of interest can be predicted as well. For instance, the result of a simulated turning circle to starboard with a rudder angle of 35° is compared with a free model test in Figure 17. The main parameters of the turning circle tests are compared in Table 6 with experiments showing good agreement. Note that the tanker fulfils the IMO recommendations with margin.

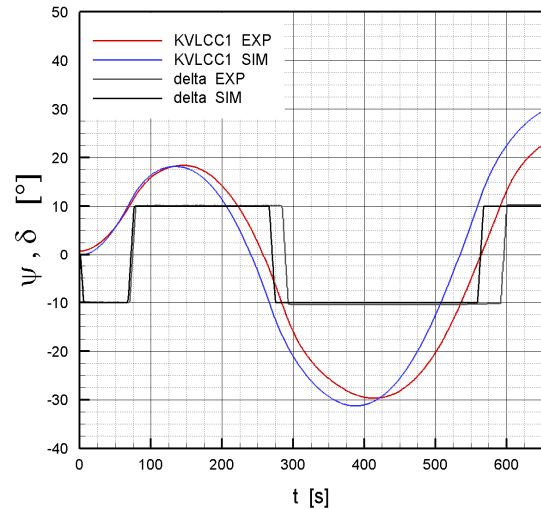


Figure 16: 10°/10° zig-zag test starting to starboard

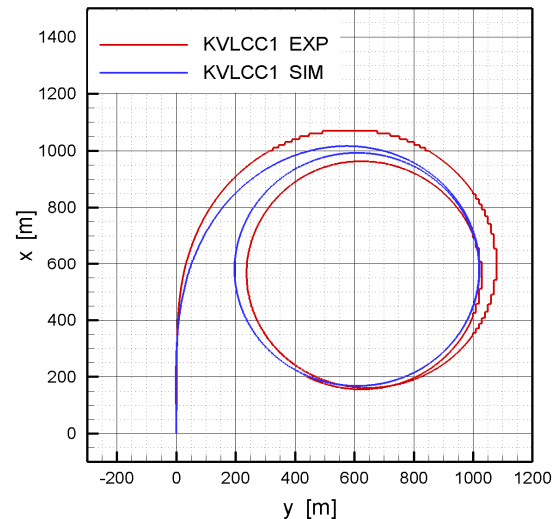



Figure 17: Turning circle test with $\delta = 35^\circ$

Table 6: Characteristic parameters of turning circle test

$\delta = -35^\circ$	SIM	EXP
x_{90° / L_{pp}	3.10	3.03
y_{180° / L_{pp}	3.13	3.25
ϕ_{st} / L_{pp}	2.58	2.44
V_{st} / V_0	0.39	0.37
r_{st} [°/s]	0.43	0.42

 INTERNATIONAL TOWING TANK CONFERENCE	ITTC – Recommended Procedures and Guidelines		7.5-03 04 - 01 Page 22 of 24	
	Guideline on Use of RANS Tools for Manoeuvring Prediction		Effective Date 2024	Revision 03

This approach has become quite common when analysing manoeuvrability using CFD. At SIMMAN 2014 many institutes were seen to use this approach with good results.


5. SYMBOLS

B	Breadth, moulded, of ship hull	(m)
C_B	Block coefficient ∇/LBT	
GM	Transverse metacentric height	(m)
I_{xx}	Roll mass moment of inertia around the principal axis x	(kg m ²)
I_{yy}	Pitch mass moment of inertia around the principal axis y	(kg·m ²)
I_{zz}	Yaw mass moment of inertia around the principal axis z	(kg·m ²)
I_{xy}	Real products of inertia in the case of non-principal axes	(kg·m ²)
I_{yz}	Real products of inertia in the case of non-principal axes	(kg·m ²)
I_{xz}	Real products of inertia in the case of non-principal axes	(kg·m ²)
i_{xx}	Roll radius of gyration around principal axis x	(m)
i_{zz}	Yaw radius of gyration around principal axis z	(m)
K	Roll moment on body, moment about body x-axis	(N·m)
L_{PP}	Length between perpendiculars	(m)
L_{CB}	Longitudinal centre of buoyancy	(-)
m	Mass	(kg)
N	Yaw moment on body, moment about body z-axis	(N·m)
r	Yaw velocity, rotational velocity about body z-axis	(1/s)
T	Draught, moulded, of ship hull	(m)
T	Period	(s)
U_0	Ship speed	(m/s)
u	Surge velocity, linear velocity along body x-axis	(m/s)
v	Sway velocity, linear velocity along body y-axis	(m/s)
X	Force in direction of body axis x	(N)
x_G^*	Longitudinal displacement of center of gravity in ship fixed coordinate system	(m)


Y	Force in direction of body axis y	(N)
z_G^*	Vertical displacement of center of gravity in ship fixed coordinate system	(m)
δ	Rudder angle	(rad)
j	Roll angle	(rad)
\dot{j}	Roll angular velocity	(rad/s)
ψ	Angle of yaw	(rad)
\dot{y}	Yaw angular velocity	(rad/s)
∇	Displacement volume	(m ³)

6. REFERENCES

- Abdel-Maksoud M., Müller V., Xing T., Toxopeus S., Stern F., Petterson K., Tormalm M., Kim S., Aram S., Gietz U., Schiller P. and Rung T. (2015), "Experimental and Numerical Investigations on Flow Characteristics of the KVLCC2 at 30° Drift Angle", 5th World Maritime Conference, Rhode Island, USA.
- Abkowitz, M.A., (1964), "Lectures on Ship Hydrodynamics - Steering and Manoeuvrability", HyA Report HY-5, Copenhagen
- Anderson, D.A, Tannehill, J.C., and Pletcher, R.H. (1984), "Computational fluid mechanics and heat transfer", Hemisphere, New York
- Aram, S., Mucha, P. (2023) "Computational Fluid Dynamics Analysis of Different Propeller Models for Ship Maneuvering in Calm Water." Ocean Engineering, 276 114226, <https://doi.org/10.1016/j.oceaneng.2023.114226>
- Bertram, V. (2012), "Practical Ship Hydrodynamics," Elsevier
- Blazek, J. (2001), "Computational Fluid Dynamics: Principles and Applications", Elsevier

 <small>INTERNATIONAL TOWING TANK CONFERENCE</small>	ITTC – Recommended Procedures and Guidelines		7.5-03 04 - 01 Page 23 of 24
	Guideline on Use of RANS Tools for Manoeuvring Prediction		Effective Date 2024 Revision 03

- Broglia, R., Durante, D., Dubbioso G. and Di Mascio, A. (2011), "Tuning Ability Characteristics Study of a Twin Screw Vessel by CFD", International Conference on Computational Methods in Marine Engineering, Lisbon, Portugal
- Carrica, P.M., Ismail, F., Hyman, M., Bhushan, S., and Stern, F. (2013), "Turn and Zigzag Maneuvers of a Surface Combatant Using a URANS approach with Dynamic Overset Grids", Journal of Marine Science and Technology, Vol. 18, No. 2, pp. 166-181
- Carrica, P., and Stern, F. (2008), "DES simulations of KVLCC1 in turn and zigzag manoeuvring with moving propeller and rudder", Proceedings SIMMAN 2008, Copenhagen
- Cebeci, T., Shao, J.R., Kafyeke, F., and Laurendeau, E. (2005), "Computational Fluid Dynamics for Engineers", Horizons Publishing
- Cura Hochbaum, A., Vogt, M., and Gatchell, S. (2008), "Manoeuvring prediction for two tankers based on RANS calculations", Proceedings SIMMAN 2008, Copenhagen
- Durante D., Broglia R. Muscari, R, and Di Mascio A., (2010), "Numerical Simulations of a Turning Circle Manoeuvre for a Fully Appended Hull", 28th ONR Symposium on Naval Hydrodynamics, Pasadena, Los Angeles, USA
- Gothenburg 2010, A Workshop on Numerical Ship Hydrodynamics <https://research.chalmers.se/en/publication/131971>
- IMO, International Maritime Organization, (2002), Resolution MSC.137(76), "Standards for Ship Manoeuvrability", London
- Ferziger, J.H., and Peric, M. (2002), "Computational Methods for Fluid Dynamics", Springer
- Franceschi A., Piaggio B., Tonelli R., Villa D., Viviani M. (2021) "Assessment of the manoeuvrability characteristics of a twin shaft naval vessel using an open-source CFD code" Journal of Marine Science and Engineering, Vol. 9 (6)
- Franceschi A., Piaggio B., Villa D., Viviani M. (2022) "Development and assessment of CFD methods to calculate propeller and hull impact on the rudder inflow for a twin-screw ship" Applied Ocean Research, Vol. 125
- Hirsch C. (1988), "Numerical computation of internal & external flows", Wiley Series in Numerical Methods in Engineering
- Hough, G. R., Ordway, D. H. (1965) "The Generalized Actuator Disk." Developments in Theoretical and Applied Mechanics, 2: 317–336
- ITTC Recommended Procedures and Guidelines. Validation and Verification of RANS Solutions in the Prediction of Manoeuvring Capabilities, No. 7.5-03-04-02
- Ji L., Sreenivas, K., Hyams, D. G., and Wilson R.V. (2010), "A Parallel Universal Mesh Deformation Scheme for Hydrodynamic Applications", 28th ONR Symposium on Naval Hydrodynamics, Pasadena, Los Angeles, USA.
- Launder, B.E., Reece, G.J. and Rodi, W. (1975), "Progress in the Development of a Reynolds-Stress Turbulent Closure.", Journal of Fluid Mechanics, Vol. 68(3), pp. 537-566.
- Launder, B.E., and Spalding, D.B. (1974), "The numerical computation of turbulent flows", Comput. Meth. in Appl. Mech. Eng. Vol.3
- Menter, F.R. (1994), "Two-Equation Eddy-Viscosity Turbulence Models for Engineering Applications", AIAA Journal, Vol.32, No.8

	ITTC – Recommended Procedures and Guidelines		7.5-03 04 - 01 Page 24 of 24
	Guideline on Use of RANS Tools for Manoeuvring Prediction		Effective Date 2024 Revision 03

Menter F.R., Kuntz M., and Langtry R., (2003), "Ten Years of Industrial Experience with the SST Turbulence Model", Turbulence, Heat and Mass Transfer 4, ed: K. Hanjalic, Y. Nagano and M Tummers, Begell House, Inc., pp. 625-632.

Muscari, R, R. Broglia and A. Di Mascio, (2008), "Trajectory Prediction of a Self-Propelled Hull by Unsteady RANS Computations", 27th ONR Symposium on Naval Hydrodynamics, Seoul.

Sadat-Hosseini, H., Wu, P.C. and Stern, F. (2014), "CFD simulations of KVLCC2 ma-

neuvering with different propeller modeling", Proceedings SIMMAN 2014, Copenhagen

SIMMAN 2008: www.simman2008.dk

SIMMAN 2020: www.simman2020.kr

Tokyo 2015 – A Workshop on CFD in Ship Hydrodynamics, www.t2015.nmri.go.jp

Wilcox, D.C. (1993), "Turbulence Modeling for CFD", DCW Industries, La Cañada, California